Synthesis of YSZ/TiO_2 core–shell feedstock powders via the air plasma spray method

Mohammad Reza Dadfar, Mohammad Reza Rahimipour ✉, *Mohammad Reza Vaezi, Abolfazl Gholamzadeh*

Materials and Energy Research Center (MERC), Karaj, P.O. Box 31787-316, Iran
✉ *E-mail: m-rahimi@merc.ac.ir*

Published in Micro & Nano Letters; Received on 18th December 2016; Revised on 17th February 2017; Accepted on 27th February 2017

The core–shell structures can improve material properties and easier material selections for applications in new purposes. In this study, yttria-stabilised zirconia (YSZ)/TiO_2 feedstock powders were synthesised via the air plasma spray method to investigate morphology changes, phase transformations and formation of core–shell structure. X-ray powder diffraction, scanning electron microscope (SEM) and EDS were used for phase analysis, morphology and core-shell characterisation, respectively. Results revealed that YSZ/TiO_2 core–shell powders can be employed using the plasma spray method. SEM images showed that entire TiO_2 nanoparticles had melted around YSZ powder. The shell thickness was estimated between 1 and 5 μm. In the plasma process the YSZ monoclinic phases transformed to the tetragonal phases, but no changes were observed in the cubic phases.

1. Introduction: In many applications such as electromagnetic, thermal barrier coatings (TBCs), electronics and catalysis, different types of powders are being used [1–3]. In some applications, the bulk properties of a powder and in some cases the surface properties of the powder are essential. TBC need to have both bulk and surface properties for thermal insulation, toughness and high temperature sintering.

The agglomerated and sintered yttria-stabilised zirconia (YSZ) powders can be melted at the surface by the air plasma spray (APS) because of its high plasma temperature (above 10,000°C) [4]. Materials have a major effect in the gas-turbine industry's requirements for improved properties such as durability and energy efficiency. There is great interest to use ceramic topcoats with better properties such as reduced high-temperature thermal conductivities [5–11]. The use of lower thermal conductivity led to improvement of TBCs durability by decreasing the metal temperature and postponing the thermally activated processes that are responsible for failure. Furthermore, engine efficiency can be improved by operating at higher temperatures. To reduce thermal conductivity at elevated temperatures, it is necessary to decrease phonon conduction and radiative heat transfer [12]. Creation of cracks and pores within the topcoat and moderation of sintering at elevated temperatures also reduce both phonon conduction and radiative heat transfer [13, 14]. Although the developing of suitable new TBC ceramics continues to incorporation of characteristics in a ceramic with lower conductivity and higher use temperature [15].

The core–shell structure is a new approach for synthesising powders with different bulk and surface properties. This structure also can affect phonon conduction and radiative heat transfer. Many core–shell structures have been synthesised up to now. Core–shell structures, such as CNTs/Fe [16], ZnO-coated iron nanocapsules [17], $SrFe_{12}O_{19}/CoFe_2O_4$ [18], $TiO_2/BaFe_{12}O_{19}$ [19], SiO_2/Fe_3O_4 [20], Fe_3O_4/polypyrrole (PPy) [21], Co/Fe_3O_4 [22], Fe/SiO_2 [23] and CdTe/CdS [24], have been fabricated by various methods.

The core–shell structure composite is very useful in applications such as catalysts, microwave absorbing materials [19], magnetism [18], optoelectronic devices, [25] and biomedicine [26]. Use of this structure in TBC is not common. Most ceramic substances used for this application have a lot of problems. Core–shell structures can improve the materials' properties and give a wider range of material selection for our purposes.

In recent years, plasma process was used to produce high density and flowable spherical powders [27]. Therefore, this study is aimed to use APS for synthesising of YSZ/TiO_2 core–shell structure. However, as we know, no work has been reported on the synthesis of core–shell powders for TBC applications.

2. Experimental: The composition and commercial characterisation of YSZ and TiO_2 nanoparticles used in this work are listed in Tables 1 and 2, respectively.

The 80%wt. YSZ-20%wt. TiO_2 composition was selected for core–shell structured powders synthesis. All YSZ powders surfaces are impregnated with carboxymethyl cellulose (CMC) adhesive and as a result the YSZ surfaces were negatively charged [28]. The reaction of TiO_2 with water is as follows

$$TiO_2 + 2H_2O = Ti^{4+} + (OH)_4^- \quad (1)$$

After hydrating TiO_2, impregnated YSZ powders with CMC were added to the titania/water solution, and then mixed for 2 h at 110 RPM. Solution temperature was increased to 70°C, and then it was dried completely. TiO_2 adhered to YSZ with non-same electrostatic charge.

All powders were sprayed in water using the air plasma spraying system equipped with METCO 3M plasma gun. The spraying processing parameters of the powder are reported in Table 3. All processing parameters for synthesis of core–shell structure are shown in Fig. 1.

The morphology of the powders was examined using a Stereo Scan S360 scanning electron microscope (SEM) and Camscan MV2300 equipped with EDS analyser. The X-ray diffraction (Philips Mode PW 3710) measurements were carried out using Cu-Ka ($\lambda = 0.154$ nm) at 40 KV and 30 mA for phase identification. Porosity analysis was carried out by Image J software.

3. Results and discussion: There are three different allotropies for ZrO_2; monoclinic, tetragonal and cubic structures. The presence of the cubic and tetragonal phases is confirmed by X-ray powder diffraction (XRD) by using (400) and (004) peaks. Figs. 2*a* and *b* shows the XRD patterns of mixed YSZ/TiO_2 and core–shell structure powders before and after spraying in water, respectively.

From these patterns observed at 20%wt. TiO_2 content, after spraying in water, the monoclinic phases transform to the tetragonal phases, while cubic phases remain almost constant. After spraying, most of the powders transform to stabilised zirconia. It has been reported [29] that the presence of 20%wt. TiO_2 in structure can improve the tetragonality of zirconia. Furthermore, use of nano

© The Institution of Engineering and Technology 2017

Table 1 Composition of YSZ and number of product producer are present in the table. Table 1. Composition and commercial characterisation of YSZ.

	Particle size, μm	PAC number
zirconia–yttria 8% stabilised powder	+15–106	2008P

Table 2 Commercial properties of TiO_2 nanoparticles

Photocatalytic standard	P25
Phases	mixed rutile/anatase phase
Average particle size	21 ± 5 nm
Specific surface	50 ± 10 m^2/g

Table 3 Processing parameters of powder spraying

Voltage	55 V
Current	500 A
Primary argon flow rate	80 SLPM
Secondary hydrogen flow rate	15 SLPM
Powder feed rate	15–20 g/min
Carrier gas flow rate	40 SLPM

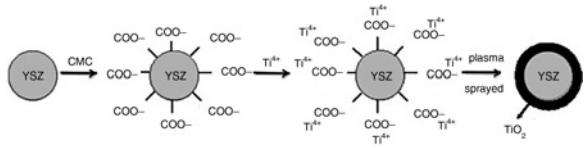

Fig. 1 *Schematic formation of the core–shell structure YSZ/TiO_2 procedure*

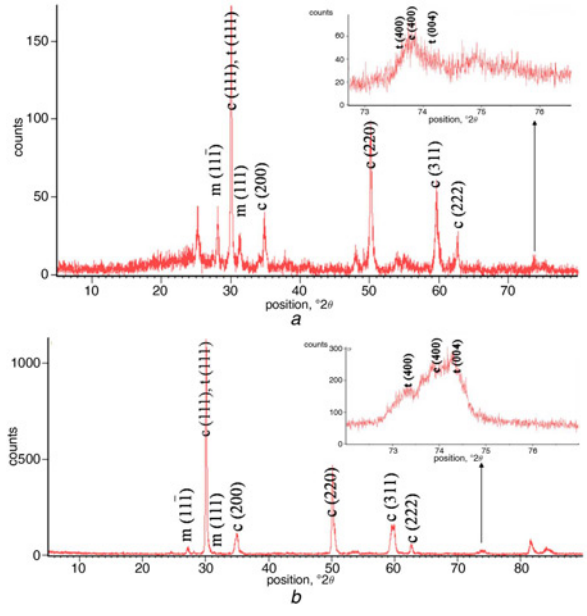

Fig. 2 *XRD pattern of*
a Mixed
b Core–shell YSZ/TiO_2 before and after spraying in water

TiO_2, due to core–shell structure, causes increase in surface contact between YSZ and TiO_2, which facilitates this process.

The operating mechanisms of Y^{3+} and Ti^{4+} doping for tetragonal stabilisation are different, however they can be complementary. The yttrium cations stabilise the tetragonal phase by widening the crystal structure and therefore the anion lattice reduces overcrowding. On the other hand, the titanium cations induce a systematic anion displacement on addition of pure zirconia [30].

The morphology of the cross-section mixed YSZ/TiO_2 powder before spraying in water is observed in Fig. 3*a*. The figure indicates that TiO_2 nanoparticles are dispersed around YSZ powder,

Fig. 3 *Morphology of the cross-section mixed YSZ/TiO_2 powder before spraying in water is observed*
a SEM image
b Map analysis
c Image *j* analysis of YSZ/TiO_2 mixture powders before spraying in water

© The Institution of Engineering and Technology 2017

doi: 10.1049/mnl.2016.0751

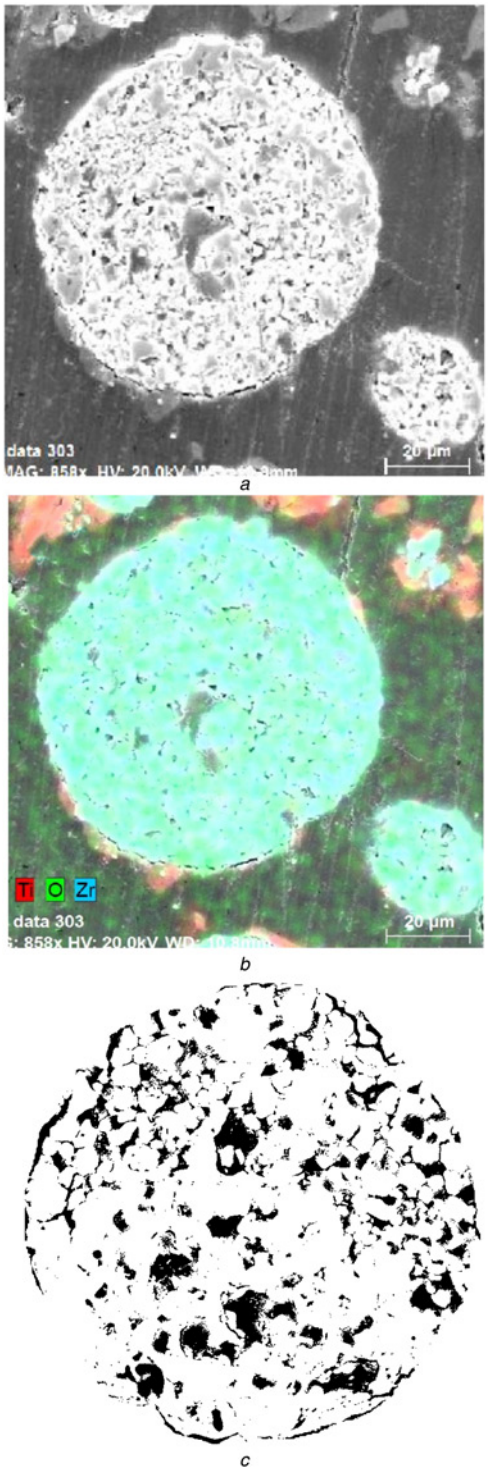

Fig. 4 *Morphology of the cross-sectional core–shell structured YSZ/TiO_2 powder after spraying in water*
a SEM image
b Map analysis
c Image *j* analysis of YSZ/TiO_2 core–shell structure powders after spraying in water

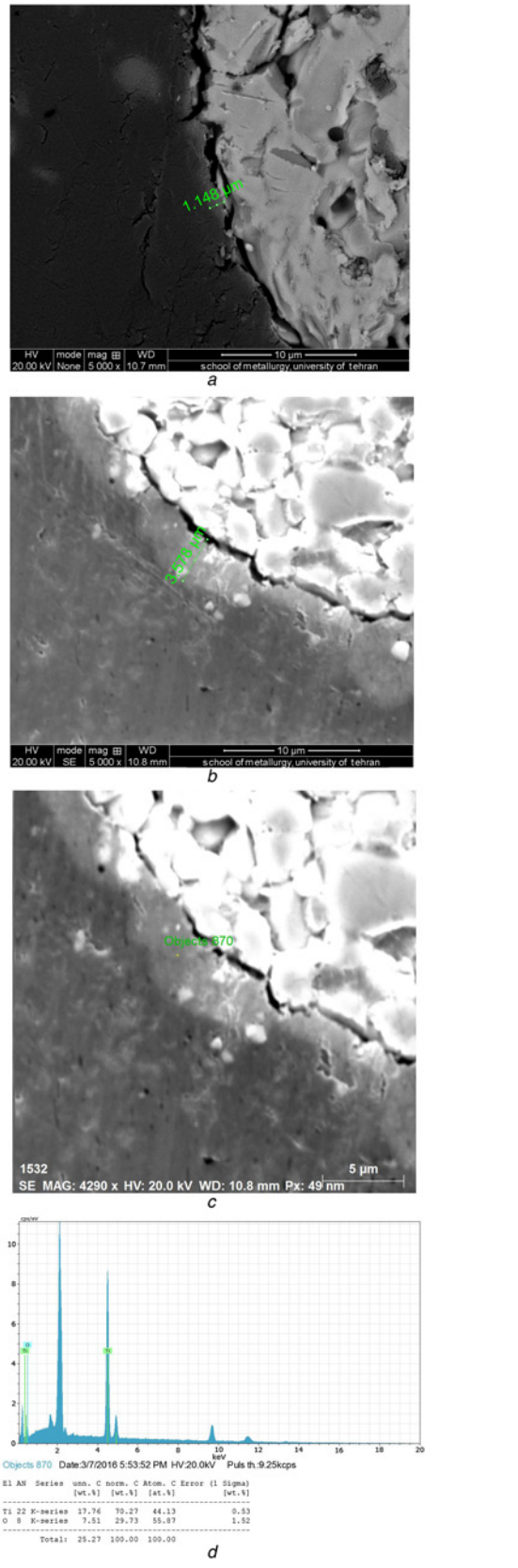

Fig. 5 *Narrow shell structure*
a Minimum thickness
b Maximum thickness
c and *d* EDS analysis of TiO_2 shell in YSZ/TiO_2 core–shell structure after spraying in water

randomly and no continuous strip between TiO_2 nanoparticles and YSZ can be observed. This result is verified by map analysis in Fig. 3*b*. 11% Porosity of YSZ powder before spraying in water was calculated by ImageJ software analysis and shown in Fig. 3*c*.

The morphology of the crosssectional core–shell structured YSZ/TiO_2 powder after spraying in water is shown in Fig. 4*a*. It can be observed that the melted TiO_2 nanoparticles are continuously shaped around YSZ powder as a strip and there is a good connection between TiO_2 nanoparticles and YSZ particles without any

© The Institution of Engineering and Technology 2017

segregation. This result is verified by map analysis in Fig. 4*b*. No obvious change of YSZ powder's porosity content after spraying in water can be observed because of the formation of a narrow and dense TiO_2 shell around YSZ (Fig. 4*c*).

Consequently, this narrow shell structure is shown in Fig. 5. The thickness of shell is between 1 and 5 µm. The EDS analysis proves that this shell is consisted of TiO_2 material. Therefore, it can be understood that impact depth of the APS process for melting the YSZ particles is very limited.

By all these experimental characterisations, it can be concluded that TiO_2 nanoparticles have good adhesion around YSZ by the method described in the experimental session. In the SEM figures, free TiO_2 nanoparticles cannot be observed and it seems that all nano particles are melted around the YSZ powders. Therefore a core–shell structure forms at high temperature of the plasma jet which is directed with a spray gun. When the powders are sprayed in water, they change to spherical shape with smooth surfaces. Moreover, the average particle size of core–shell structure after spraying in water increased from 20 ± 3 to 30 ± 5 µm. By comparing SEM images, EDS and map analysis, it can be claimed that core–shell structure of YSZ/TiO_2 has been successfully formed. For this reason, cross sections of powders before and after spraying in water are under investigations.

4. Acknowledgments: The authors acknowledge Materials and Energy Research Center, for providing financial support and A. Asjodi who support the APS process.

5 References

[1] Eslamian M., Ashgriz N.: 'Effect of precursor, ambient pressure, and temperature on the morphology, crystallinity, and decomposition of powders prepared by spray pyrolysis and drying', *Powder Technol.*, 2006, **167**, pp. 149–159

[2] Singh K., Ohlan A., Bakhshia A.K., *ET AL.*: 'Synthesis of conducting ferromagnetic nanocomposite with improved microwave absorption properties', *Mater. Chem. Phys.*, 2010, **119**, p. 201

[3] Tian S., Liu J., Zhu T., *ET AL.*: 'Polyaniline doped with modified gold nanoparticles and its electrochemical properties in neutral aqueous solution', *Chem. Mater.*, 2004, **16**, p. 4103

[4] Zhang X., Zhou K., Chang F., *ET AL.*: 'Yttria-stabilized-zirconia hollow spheres prepared by atmosphericplasma spray', *Particuology*, 2014, **14**, pp. 57–62

[5] Leyens C., Metallkd Z.: 'Accelerators TBC failure by making the top coat less strain tolerance', 2001, **92**, p. 762

[6] Padture N.P., Gell M., Klemens P.G.: 'Ceramic materials for thermal barrier coatings'. U.S. Patent No. 6,015,630, 2000

[7] Pakseresht A.H., Rahimipour M.R., Alizadeh M., *ET AL.*: 'Concept of advanced thermal barrier functional coatings in high temperature engineering components', 'Research perspectives on functional micro- and nanoscale coatings', 2016, Ch. 15, p. 396

[8] Pakseresht A.H., Javadi A.H., Ghasali E., *ET AL.*: 'Evaluation of hot corrosion behavior of plasma sprayed thermal barrier coatings with graded intermediate layer and double ceramic top layer', *Surface Coat. Technol.*, 2016, **288**, pp. 36–45

[9] Pakseresht A.H., Javadi A.H., Bahrami M., *ET AL.*: 'Investigation of microstructure and hot corrosion resistance of thermal barrier functional coating produced by spark plasma sintering method and compare with sprayed one', *Ceram. Int.*, 2016, **42**, (2), pp. 2770–2779

[10] Pakseresht A.H., Rahimipour M.R., Vaezi M.R., *ET AL.*: 'Effect of morphology and nonbounded interface on dielectric properties of plasma sprayed $BaTiO_3$ Coating', *J. Adv. Mater. Process.*, 2014, **2**, (4), pp. 25–32

[11] Pakseresht A.H., Rahimipour M.R., Vaezi M.R., *ET AL.*: 'Effect of splat morphology on microstructure and dielectric property of plasma sprayed Barium titanate films', *Appl. Surf. Sci.*, 2015, **324**, pp. 797–806

[12] Klemens P.G., Wills K.E., Dinwiddie R.B., *ET AL.* (Eds): 'Thermal Conductivity 23' (Technomics, Lancaster, PA, 1993), vol. 23, p. 209

[13] Dorvaux J.-M., Lavigne O., Mevrel R., *ET AL.*: Proc. 85th Meeting Advisory Group Aerospace Research and Development, Structures and Materials Panel, 15 – 16 October 1997, Neuilly-sur-Seine, France, 1998, p. 13

[14] Schlichting K.W., Padture N.P., Klemens P.G.: 'Thermal conductivity of dense and porous yttria-stabilized zirconia', *J. Mater. Sci.*, 2001, **36**, p. 3003

[15] Padture N.P., Gell M., Jordan E.H.: 'Thermal barrier coatings for gas-turbine engine applications', *Science*, 2002, **296**, pp. 280–284

[16] Che R.C., Peng L.M., Duan X.F., *ET AL.*: 'Microwave absorption enhancement and complex permittivity and permeability of Fe encapsulated within carbon nanotubes', *Adv. Mater.*, 2004, **16**, pp. 401–405

[17] Liu X.G., Geng Y.D., Meng H., *ET AL.*: 'Microwave-absorption properties of ZnO-coated iron nanocapsules', *Appl. Phys. Lett.*, 2008, **92**, p. 173117

[18] Zhang L., Li Z.: 'Synthesis and characterization of $SrFe_{12}O_{19}$/$CoFe_2O_4$ nanocomposites with core-shell structure', *J. Alloys Compd.*, 2009, **469**, pp. 422–426

[19] Tang X., Zhao B.Y., Tian Q., *ET AL.*: 'Synthesis, characterization and microwave absorption properties of titania-coated barium ferrite composites', *J. Phys. Chem. Solids*, 2006, **67**, pp. 2442–2447

[20] Liu B., Xie W., Wang D., *ET AL.*: 'Preparation and characterization of magnetic luminescent nanocomposite particles', *Mater. Lett.*, 2008, **62**, pp. 3014–3017

[21] Li Y., Chen G., Li Q., *ET AL.*: 'Facile synthesis, magnetic and microwave absorption properties of Fe_3O_4/polypyrrole core/shell nanocomposite', *J. Alloys Compd.*, 2011, **509**, pp. 4104–4107

[22] Wang G., Chang Y., Wang L., *ET AL.*: 'Synthesis, characterization and microwave absorption properties of Fe_3O_4/Co core/shell-type nanoparticles', *Adv. Powder Technol.*, 2012, **23**, (6), pp. 861–865

[23] Tang N.J., Jiang H.Y., Zhong W., *ET AL.*: 'Synthesis and magnetic properties of Fe/SiO_2 nanocomposites prepared by a sol–gel method combined with hydrogen reduction', *J. Alloys Compd.*, 2006, **419**, pp. 145–148

[24] Bao H., Gong Y., Li Z., *ET AL.*: 'Enhancement effect of illumination on the photoluminescence of water-soluble CdTe nanocrystals: toward highly fluorescent CdTe/CdS core-shell structure', *Chem. Mater.*, 2004, **16**, pp. 3853–3859

[25] Tamil Selvan S., Patra P.K., Ang C.Y., *ET AL.*: 'Synthesis of silica-coated semiconductor and magnetic quantum dots and their use in the imaging of live cells', *Angew. Chem. Int. Ed.*, 2007, **40**, p. 1

[26] Wuang S.C., Neoh K.G., Kang E.T.: 'Synthesis and functionalization of polypyrrole-Fe_3O_4 nanoparticles for applications in biomedicine', *J. Mater. Chem.*, 2007, **17**, p. 3354

[27] Padmanabhan P.V.A., Ramanathan S., Sreekumar K.P., *ET AL.*: 'Synthesis of thermal spray grade yttrium oxide powder and its application for plasma spray deposition', *Mater. Chem. Phys.*, 2007, **106**, pp. 416–421

[28] Wang J., Somasundaran P.: 'Adsorption and conformation of carboxymethyl cellulose at solid–liquid interfaces using spectroscopic, AFM and allied techniques', *J. Colloid Interface Sci.*, 2005, **291**, pp. 75–83

[29] Krogstad J.A., Lepple M., Levi C.G.: 'Opportunities for improved TBC durability in the CeO_2–TiO_2–ZrO_2 system', *Surf. Coat. Technol.*, 2013, **221**, pp. 44–52

[30] Li P., Chen I.W., Penner-Hahn J.E.: 'Effect of dopants on zirconia stabilization – An x-ray-absorption study: II. Tetravalent dopants' *J. Am. Ceram. Soc.*, 1994, **77**, pp. 1281–1288

© The Institution of Engineering and Technology 2017

doi: 10.1049/mnl.2016.0751